Structure and stability of semiconductor tip apexes for atomic force microscopy

P Pou[1], S A Ghasemi[2], P Jelinek[3], T Lenosky[4], S Goedecker[2] and R Perez[1]

[1] Departamento de Fisica Teorica de la Materia Condensada, Universidad Autonoma de Madrid, E-28049 Madrid, Spain
[2] Department of Physics, University of Basel, Switzerland
[3] Institute of Physics, Academy of Sciences of the Czech Republic, Cukrovarnicka 10, 1862 53, Prague, Czech Republic
[4] Department of Materials Science and Engineering, Ohio State University, Columbus, OH 43210, USA

E-mail: pablo.pou@uam.es

Abstract

The short range force between the tip and the surface atoms, that is responsible for atomic-scale contrast in atomic force microscopy (AFM), is mainly controlled by the tip apex. Thus, the ability to image, manipulate and chemically identify single atoms in semiconductor surfaces is ultimately determined by the apex structure and its composition. Here we present a detailed and systematic study of the most common structures that can be expected at the apex of the Si tips used in experiments. We tackle the determination of the structure and stability of Si tips with three different approaches: (i) first principles simulations of small tip apexes; (ii) simulated annealing of a Si cluster; and (iii) a minima hopping study of large Si tips. We have probed the tip apexes by making atomic contacts between the tips and then compared force–distance curves with the experimental short range forces obtained with dynamic force spectroscopy. The main conclusion is that although there are multiple stable solutions for the atomically sharp tip apexes, they can be grouped into a few types with characteristic atomic structures and properties. We also show that the structure of the last atomic layers in a tip apex can be both crystalline and amorphous. We corroborate that the atomically sharp tips are thermodynamically stable and that the tip–surface interaction helps to produce the atomic protrusion needed to get atomic resolution.

M This article features online multimedia enhancements

(Some figures in this article are in colour only in the electronic version)

1. Introduction

Dynamic atomic force microscopy using the frequency-modulation operation mode (FM-AFM), usually known as non-contact AFM (NCAFM), has fulfilled the long standing goal of achieving atomic resolution in all kinds of surfaces [1–3]. While imaging in this mode, the cantilever is kept oscillating with a constant amplitude at its current resonance frequency. The resonance frequency is modulated by the tip–sample interaction, that depends strongly on the distance between the tip and the sample.

A surface scan at a constant frequency shift provides images with true atomic resolution. The atomic contrast in semiconductor surfaces is associated with the interaction of a dangling bond at the very end of the tip apex with the surface dangling bonds [4, 5]. The force acting between the tip and the surface can be obtained from the experiments by performing dynamic force spectroscopy (DFS) [6–8]. Recently, this technique has been used to map the potential energy landscape of surfaces with atomic resolution [9, 10]. The dissipation signal, the energy required to keep the amplitude constant at each pixel of the image, also

provides atomic contrast [11, 12]. The FM-AFM is rapidly developing outstanding capabilities beyond imaging that rely on the precise control of the short range tip–sample force. Atom-by-atom manipulations on semiconductor surfaces with sophisticated nanostructuring [13–16] and also manipulations on insulator systems [17, 18] have been performed under room temperature (RT) conditions. Recently, chemical identification of individual surface atoms in semiconductor systems at RT [19] has been achieved in terms of differences in the maximum attractive force.

The atomic resolution and the interaction between the surface and the tip on semiconductor surfaces have been quantitatively explained by making simple assumptions about the structure of the tip apex outermost atoms [2, 4, 6, 20]. The subatomic resolution reported in the Si(111)-7 × 7 surface has been associated with a particular Si tip structure which is terminated by an atom with two dangling bonds [21, 22]. Different tip apex terminations, leading to positive or negative local electrostatic potentials, have also been proposed to explain the imaging mechanism on insulator surfaces [23–26].

Recent experimental advances in DFS [8, 27] allowed a reproducible and accurate determination of the SR tip–surface interaction even at RT. The combination of these detailed results with theoretical simulations has opened a new exciting panorama for the characterization of the tip structure. Using this approach, Hoffmann *et al* [7] have characterized the polarity of the tip termination and determined which of the two sublattices in an alkali halide (100) surface was imaged. Taking into account also quantitative dissipation spectroscopy results, it is possible to go a step further and identify the detailed structure of the tip apex. A recent series of experiments on the Ge(111)-c(2 × 8) reconstruction revealed the systematic presence of two different contrast patterns in both the frequency shift and dissipation images [28]. In the first case, rest-atoms were clearly resolved in the topography and the dissipation image showed a strong contrast on the ad-atoms. In the second case, they obtained the usual topography image where only the ad-atoms are resolved and no significant contrast in the dissipation signal. These results were attributed to two different tip apex structures, as they were able to switch between these two contrast patterns during the same experimental session with just a gentle contact between the tip and the surface. Large-scale first principles simulations for more than 30 different candidates showed that forces and dissipation energies on different sites of the unit cell can be quantitatively matched by two different terminations: (a) a dimer-like structure of Ge atoms (similar to the dimer Si tip shown in figure 1(a)) and (b) a Ge T4-like apex (like the one in figure 1(a)).

The extreme sensitivity of the topographic images and the dissipation signals to the tip apex structure, and the ability to reproduce quantitatively these results with certain configurations of the outermost atoms in the apex seem to provide a quite convincing argument to assume that those are the real sharp nanostructures found in the experimental tip. However, a more fundamental approach is needed in order to demonstrate that these are optimal, stable structures that are naturally formed during the experimental tip preparation.

(a)

Tip H3   Tip T4   Tip dimer

(b)
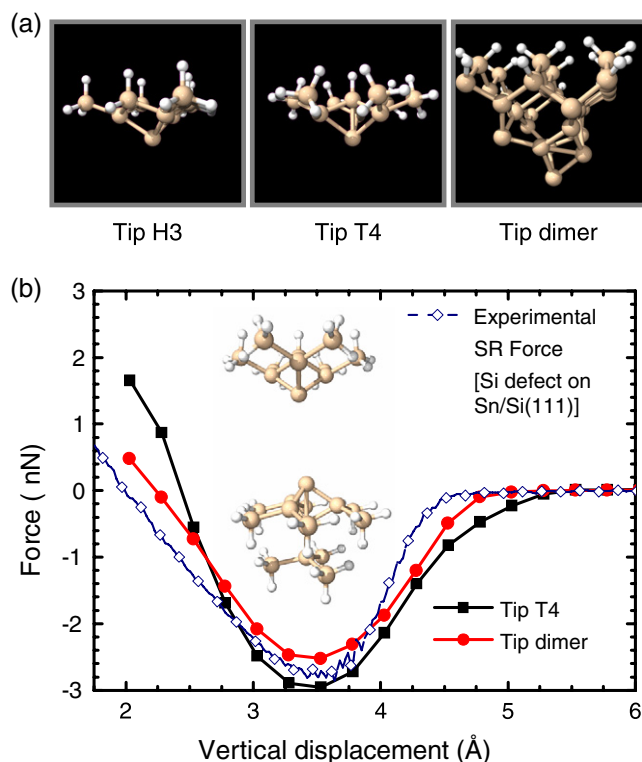
Figure 1. (a) Ball-and-stick models of the 3 small tip apexes introduced in previous works based on semiconductor surface reconstruction criteria, we have called them H3, T4 and dimer tips due to the similarity with those atom surface configurations. (b) Force as a function of the separation for the interaction between the T4 (solid black squares) and the dimer (solid red circles) tips with a cluster simulating a Si surface ad-atom (inset). The calculation has been done with the Fireball code [30]. For comparison, we also plot an experimental short range force (open blue diamonds) over a Si substitutional defect in a Sn/Si(111)-($\sqrt{3} \times \sqrt{3}$)R30° surface (for details see [29]). The reference of the experimental vertical displacement has been chosen to make the minima coincide.

Moreover, it is clear that these small models cannot explain some important properties of the tip–sample interaction. For example, DFS experiments on the Sn/Si(111)-($\sqrt{3} \times \sqrt{3}$) surface show significant variations in the shape of the SR force curves measured over the same surface ad-atom with the tips used [19, 29], particularly in the repulsive regime. These variations indicate very different elastic responses of the tip under the applied stress, that depend not only on the outermost apex atoms but also on the structure of the last few nanometres of the tip. Notice that these mechanical properties also play an important role in the atomic manipulations taking place in the repulsive regime [13, 16].

In the experiments, the atomic structure of the apexes is determined not only by the tip preparation previous to the measurement sessions but also by the processes that take place during the measurements. The whole experimental preparation of tips is one of the most delicate steps. There are some 'rules of thumb' which are more or less followed in most of the experiments. The tips, mostly made from silicon and exposing oxidized surfaces, are usually cleaned by ion sputtering and annealed. After this procedure, some tips yield

atomic resolution but more often several scans over a surface region are required to get atomic contrast. In some cases even a gentle indentation is needed. During the scan or the indentation process the tip could strongly interact with the surface producing a transfer of atoms between the surface and the apex. The tip–surface interaction could also modify the atomic structure of the tip generating the atomic protrusion without any atom transfer between the tip and the surface.

The main goal of this work is to identify the most common realistic atomic structures of the sharp apexes needed for high-resolution force spectroscopy and imaging. In this study, two considerations should be taken into account: (a) the intrinsic thermodynamic stability of the atomically sharp tips, i.e., can these tips be a result of the sputtering and annealing process and can they be thermodynamically stable?; and (b) the sharpening and contamination processes due to the tip–surface interaction.

This is a very challenging theoretical problem, as the lack of experimental information leaves many variables unknown in a large system with a very complex energy landscape. Our proposal to tackle this problem is to combine several simulation approaches, that balance accuracy and efficiency with system size, to identify stable and realistic structures. We have performed calculations ranging from the detailed study of very small tip terminations with less than 50 atoms to an extensive search of local energy minima in systems with more than 400 atoms. We have analysed not only the atomic and electronic structure of the tip apex, and its mechanical and thermal stability, but also the effect of the interaction with the surface atoms in order to answer three basic questions: (i) the structure of the tip outermost atoms, (ii) the influence of the last few atomic layers of the tip, and (iii) the role of possible sharpening processes.

For this study, we have chosen silicon as the prototypical tip material and focused on experiments on semiconductor surfaces. There are two main reasons for this election: (a) silicon is the base material in most of the tips used in the experiments; and (b) although the tip can be contaminated by surface materials, the main characteristics of the apexes are determined by the common properties shared by the atoms that form semiconductor materials.

The rest of the paper is organized as follows: after this introduction, we present the methods used in the calculations (section 2). Then, we introduce the different systems we have simulated and discuss the results trying to answer the three questions posed above (section 3). We finish with the conclusions (section 4).

2. Methods

We have studied several systems with different boundary conditions and different calculation methods to collect extensive information for a reliable characterization of realistic tip structures.

In order to get a good description of the tip terminations, their atomic and electronic structure and also their interaction with the surface, accurate *ab initio* DFT methods [31, 32] are the best choice. For this task, we have used the Fireball

code [30, 33]. This local orbital DFT method employs numeric atomic orbitals with a finite extension (Fireballs [34]) and introduces a series of approximations in the charge self-consistency and the evaluation of the exchange correlation functional in order to drastically reduce the computational time (compared not only to plane-wave methods but also to other approaches based on a local orbital basis), but still keeping a good accuracy in the results. The calculations presented in this paper are performed within the LDA [35]. We have used a minimal basis set that includes s and p orbitals for Si with the following cutoff radii: R_C (Si s orbital) $= 4.8$ au, R_C (Si p orbital) $= 5.4$ au. This basis set yields a very good description of the bulk properties of Si: a lattice parameter $A = 5.46$ Å and a bulk modulus $B = 105$ GPa, compared to the experimental values $A = 5.43$ Å, $B = 100$ GPa. This basis set also describes accurately different Si surfaces. In particular, both the Si(111)-7 × 7 and the Si(100)-2 × 1 reconstructions are stable and their geometries compare well with standard plane-wave calculations. For example, our height difference between a corner and a central ad-atom in the faulted unit cell of the Si(111)-7 × 7 structure $\Delta d = 0.06$ Å, and the characteristic dimers of the Si(100)-2 × 1 have a length of $d_{dimer} = 2.37$ Å and a tilted angle $\alpha = 23°$. Plane-wave DFT-LDA calculations [36] give $\Delta d = 0.05$ Å, $d_{dimer} = 2.32$ Å and $\alpha = 18°$. This basis set has been successfully used in our calculations for chemical identification and single atom manipulation with the FM-AFM [15, 16, 19].

This is the method that we have applied in our study of the different small tip apexes (less than 50 atoms, section 3.1) and the larger Si cluster (71 atoms, section 3.2). We have also used it to test some of the tip configurations obtained for the very large system (434 atoms) described with a tight-binding approach (see below and section 3.3). In all of these calculations we have used a supercell approach and considered only the Γ point to sample the Brillouin zone. The convergence criteria for the total energy and forces are 10^{-6} eV and 0.05 eV Å^{-1} respectively. The SR forces were calculated as a numerical derivative of the total energy versus distance curve.

The systematic search for stable, low energy tip structures requires the systematic exploration of the complex energy landscape of a large system with realistic boundary conditions. We have performed this study with the minima hopping method (MHM) introduced by Goedecker [37]. This method tries to find the global energy minimum by exploring the phase space with the following strategy: a feedback mechanism uses information from the already collected history list to make more vigorous escape attempts when the algorithm is revisiting previously found minima, thereby preventing the algorithm from getting trapped in an incorrect minimum. In this way the chance to visit a configuration is reduced but it still allows us to visit important configurations such as those needed to easily cross energy barriers which open doors to other regions of the configurational space.

The system size (more than 400 atoms) and the number of calculations required to perform an adequate exploration of the configurational phase space prevent us from using *ab initio* methods. The large hydrogenated silicon system studied with
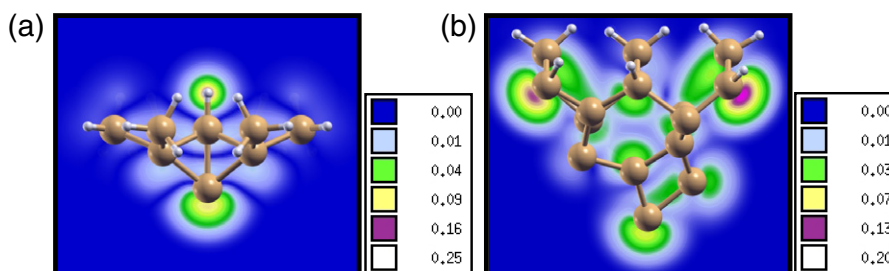
Figure 2. Projected electronic charge density of (a) the T4 tip and (b) the dimer tip. To visualize the dangling bond states (which are close to the Fermi level), the charge density has been calculated in both cases for the eigenstates in the energy range between the Fermi level and 1 eV below. Notice that the isolines do not follow a linear scale, but they follow a square root scale to enhance the resolution.

the MHM has been described with a tight-binding scheme of the Lenosky type [38]. The pair potential and the tight-binding matrix elements are represented by cubic splines with a 5.24 Å fixed radial cutoff in order to allow maximum flexibility. The spline parameters were fitted to *ab initio* force and energy data of silicon–hydrogen clusters, bulk silicon, the hydrogen molecule and a silane dimer. The cluster database consists of 40 SiH clusters having 10, 11 or 14 silicon atoms and 1–16 hydrogen atoms. The reference energies and forces used for the fitting were obtained from a plane-wave density functional calculation using the local density approximation (LDA) [35] and the Perdew, Burke and Ernzerhof (PBE) functional [39]. This tight-binding describes with good accuracy the properties of bulk Si, Si clusters and the Si surfaces. Both the Si(111)-7×7 and the Si(100)-2×1 reconstructions are stable (for example, it yields the following solutions for the geometrical parameters compared above: $\Delta d = 0.05$ Å, $d_{dimer} = 2.37$ Å and $\alpha = 13°$). This method has allowed us to do a fast search of low energy configurations of tip structures. In order to further confirm the tight-binding results, we have recalculated with Fireball some of the stable configurations found and tested their performance upon interaction with the surface.

3. Results and discussion

3.1. Small tip apexes

Firstly, we discuss the small tips, formed by up to 50 atoms, introduced to describe the configuration of the outermost atoms of the tip. These small tip apexes (shown in figure 1(a)) were derived from the known stable semiconductor surface terminations: notice that the H3 tip is based on a rest-atom of a reconstructed (111) surface, T4 is related to an ad-atom configuration, and the dimer structure resembles the dimers of a reconstructed (100) surface. Semiconductor tip models based on these structures, but with different chemical compositions including pure Si tips, pure Ge tips, and Si tips contaminated with surface material (Sn, Ge, etc), were used in previous studies [2, 3, 19, 25, 26, 28, 40] in order to explain the experimental observations.

Figure 1(b) shows the interaction of two of these tips (the T4 and the dimer-like structure) with a small cluster which mimics well a surface Si ad-atom (see the ball-and-stick model in figure 1(b)). For comparison, we have also included the

experimental SR force versus distance curve measured over a Si substitutional defect in the Sn/Si(111)-$(\sqrt{3} \times \sqrt{3})$R30° surface [29]. The H3 tip provides almost identical results to the T4 tip. The theoretical force curves for both tips capture the basic features of the experimental SR forces in that system, but there are clear differences in both the attractive and the repulsive regime. These calculations show that the details of the interaction between the tip and the surface depend strongly on the structure of the tip termination: a change in the neighbourhood of the outermost tip atom produces a variation of the minimum force value larger than 10%.

The detailed study of both the conservative and dissipative part of the interaction between Ge tips and the Ge(111)-c(2×8) reconstruction (see [28]) showed that the H3 and T4 structures have a qualitatively different behaviour compared to the dimer tips. The corresponding Si tips displayed the same behaviour, that can be easily understood in terms of their electronic structure. H3 and T4 tips are characterized by a single outermost atom which has a dangling bond (figure 2(a)). The neighbouring Si atoms in the tip second layer have a four-fold coordination that saturates all of their possible bonds. On the other hand, the dimer tip has a much more open structure that is characterized by the presence of two atoms, each of them with a dangling bond (figure 2(b)). These two dangling bonds strongly interact between themselves and with the dangling bonds in the surrounding atoms. This interaction modifies the charge state of these dangling bonds, inducing a charge transfer to the outermost atom in the tip from the other atom in the dimer in order to minimize the total energy. This subtle energy balance can be altered by the interaction with the surface, changing the charge distribution and the dimer structure. This process is analogous to the one that stabilizes the tilted dimers of the Si(100) surface reconstruction. This flexibility explains some of the features in the force curves. The range of the interaction is larger on the T4 tip due to the favourable orientation of its dangling bond, that it is pointing to the surface and interacts with the dangling bond of the Si ad-atom, that is also normal to the surface. In the case of the dimer tip, the unfavourable initial orientation of the dangling bond in the outermost atom can be overcome by a modification of the dimer structure associated with a charge transfer once the tip–sample interaction is large enough. This 'sharpening' effect leads to the rapid variation of the force in the 4.25–4.75 Å distance range and explains the ability of the

dimer tip to resolve the rest-atoms in the Ge(111)-c(2 × 8) reconstruction [28]. Apparently quite sharp tips such as the T4 and H3 structures cannot resolve the rest-atoms because when located right on top of a rest-atom, the atoms on the tip second layer interact with the ad-atoms surrounding the rest-atom. However, in the case of the dimer tip, the sharpening effect associated with the flexible charge transfer and the reduced coordination of the atoms in the dimer, results in that interaction with the surrounding ad-atoms starting at much closer tip–surface distances. The flexibility associated with the dimer structure is also responsible for the strong hysteretic behaviour of the force curve (leading to an energy dissipation of 0.8 eV/cycle) discussed in [28].

The variation of the maximum SR attractive force (F_{max}) among the different tip structures discussed above is still small compared to the one observed in experiments (see, for example, [19]). In order to understand the origin of this large dispersion, we have explored the role of the chemical composition of the tip. We have calculated the interaction of several Sn-contaminated Si dimer tips with the Si cluster mimicking the surface. The results, summarized in figure 3, reveal the strong dependence of F_{max} on the chemical nature of the outermost atom. In particular, we observe a difference of F_{max} values larger than 30% between the Si and Sn terminated tips. On the other hand, the presence of an isovalent Sn impurity in any other position different from the outermost atom of the apex—including the case where the Sn replaces the other Si atom in the dimer—induces only a small variation in F_{max}. These results point out the localized character of the tip–sample interaction, that is associated with the strong spatial localization of the dangling bonds in semiconductor systems [2] and reveal that F_{max} is dominated by the chemical nature of the tip apex atom and the outermost surface ad-atom.

The H3, T4 and dimer terminations are mechanically stable under quite large applied loads, even in the presence of contaminating isovalent atoms. In this context, we define mechanical stability as the capability of a tip to recover its original atomic configuration after a strong interaction with the surface. In this sense, all of these tips can provide stable imaging and, therefore, are very good candidates to represent the real tip terminations in the experiments showing atomically-resolved images on semiconductor surfaces.

One may wonder if the strict boundary conditions imposed in these small nanoasperities are actually controlling their stability. The limited size implies that most of the tip atoms, in fact all of them apart from the 4–6 outermost atoms in the apex, are fixed in the positions given by the bulk geometry and their dangling bonds are saturated with hydrogens in order to mimic the tip continuation. It may well be that this 'crystallinity' that we are enforcing in the last tip layers is responsible for the stability of these particular structures. In order to assess this issue we need to consider larger systems such as the ones described in the following sections.
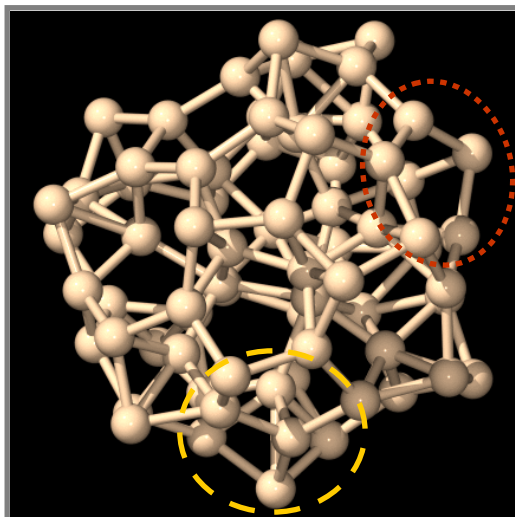
3.2. Si cluster

In order to check the stability of the small tip apexes discussed above, we have investigated the structure of a larger cluster
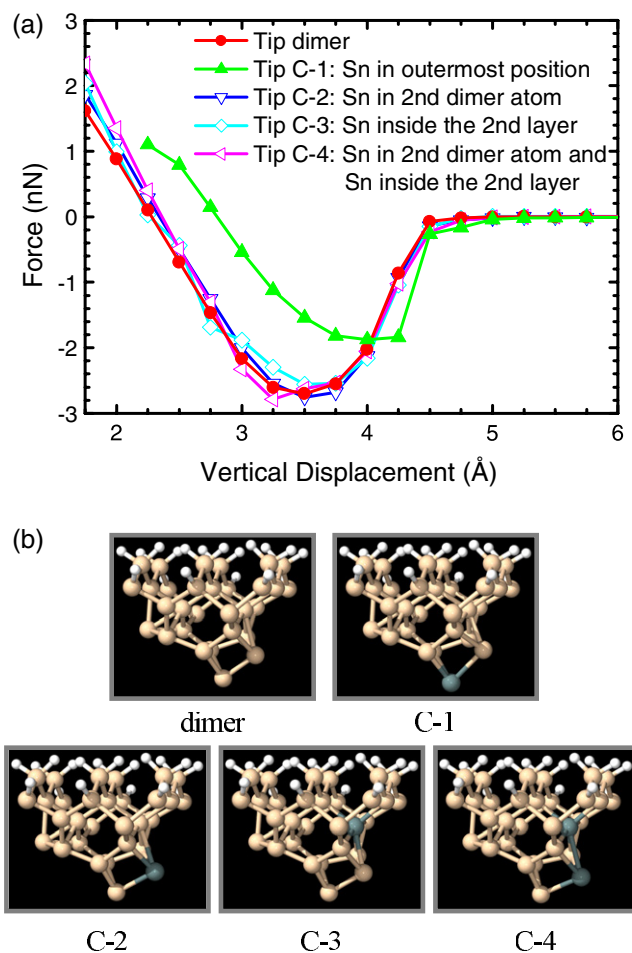
Figure 3. Force as a function of the separation for the interaction between a cluster that simulates a Si ad-atom and tips contaminated with Sn atoms in different positions: Sn atom in the outermost position (solid green triangles, C-1 in the ball-and-stick model shown in b), Sn atom in the other position of the dimer (open blue down-triangles, C-2), a Sn atom inside the second layer (open cyan diamonds, C-3), and a Sn atom in the dimer and another one inside the second layer (open magenta left-triangles, C-4). We also plot the force for the Si dimer tip (solid red circles, dimer).

of Si atoms. This system has boundary conditions that are completely different from the ones in the nanoasperities as all of the atoms are free to move in order to find the ground state configuration. Thus, this study will provide information not only about the possible atomic tip terminations but also about the structure of the atomic layers that connect the outermost apex atoms with the rest of the tip.

Si clusters have been the subject of a great research effort during the last few years (see, for example, [41]). Clusters with less than 100 atoms can still be simulated by *ab initio* methods, but the complexity associated with the large number of degrees of freedom makes the determination of the exact ground state a theoretical challenge. We have performed a simulated annealing of a cluster with 71 Si atoms using the Fireball code. In the first step of this process, we heat up the system by performing a molecular dynamics simulation on the NVE scheme at a temperature of 1000 K in order to allow the exploration of a large part of the phase space. The removal of

Figure 4. (a) Ball-and-stick model of a Si cluster with 71 atoms. The atomic structure corresponds with a local minimum obtained with simulated annealing. We have highlighted a T4 (yellow dashed line) and a dimer (red dotted line) termination.

energy during the annealing brings the system to a low energy configuration close to the global minimum. The determination of the exact ground state is a complex task that would require to repeat this process many times in order to start the annealing in very different regions of the phase space. This complex minimization is not necessary in our case as the qualitative features of the cluster structure are shared by most of the low energy configurations, including the global minimum.

Figure 4 displays the atomic structure corresponding to a local energy minimum of our cluster with 71 Si atoms. This configuration is representative of the structure of Si clusters with a similar number of atoms. In particular, it shows the main features found in other published structures [41–44]: the core of the cluster is in an amorphous configuration with atoms that have a coordination number larger than 4; this core is surrounded by an outer layer that shows the same atomic local structures that are characteristic of the different Si surface reconstructions. The analysis of this outer layer provides valuable information about the possible terminations of tip apexes. Zooming in the atomic protrusions, we can easily identify T4 or dimer terminations (see, for example, the atoms highlighted in figure 4). Most of the sharper protrusions indeed coincide with the small apex structures of figure 1(a).

Experiments and simulations show that the inner core of Si clusters with less than several hundreds of atoms is amorphous [41], the configuration presented here being just an example. Notice that, even in the presence of that amorphous core, we still see the same tip terminations. Therefore, this study confirms that the H3, T4 and dimer-like structures are stable and representative of the atomic terminations that we can expect in semiconductor systems. Besides, it also shows that atomically sharp apexes can naturally appear during the tip cleaning process (involving ion-bombardment and annealing steps) without the need of a gentle nanoindentation on the surface.

The cluster calculation offers some information about the intermediate configuration of the tip, i.e., the structure of the

last (2–10) atomic layers: one would expect this configuration to be similar to the inner structures of these clusters. This configuration depends on the cluster size: while small clusters are always amorphous (as in the case shown in figure 4), larger clusters show a crystalline core. Both the experimental and the theoretical evidence indicates that the transition to crystalline structures takes place around $N = 400$ atoms [41]. Therefore, the character of the intermediate tip structure cannot be confirmed by the cluster calculation. In clusters, the relative stability of these configurations is controlled by the bulk-surface ratio, due to the open boundary conditions. It is not clear if this is the best model to represent the real tip apex, where the structure of the last hundreds of atoms must be constrained by the crystalline macroscopic part of the tip. We will try to solve these limitations in system size and in the implementation of the correct boundary conditions with the last system considered in this work.

3.3. Si pyramid on Si(100)

In order to complete our study of tip apex structures, we have tackled the calculation of a larger system with more realistic boundary conditions: a small Si cluster (50 atoms) with a pyramidal shape attached to a Si(100) surface (see the initial configuration in figure 5(b)). The system size is large enough to allow the atoms of the initial Si pyramid to relax and adopt any stable, low energy configuration, including the possibility to leave the cluster and diffuse towards the surface. We have used a slab with 4 atomic layers and an 8×8 surface unit cell (total size: 30.7 Å × 30.7 Å). The total number of atoms in the system (including the Si pyramid) is 434. Only the atoms of the last atomic layer at the bottom of the slab and the hydrogens which saturate their dangling bonds are fixed during the search for the low energy structures. To characterize this system we have used the minima hopping method [37]. Due to the system size and to the large number of calculations required, we have used a tight-binding approach for the electronic and mechanical properties of Si, as described in section 2.

The minima hopping method provides an exhaustive, systematic exploration of the energy landscape in order to identify the relevant, low energy local minima. More than 12 000 low energy local minima have been collected during our study. In figure 5(a), we plot the energy for a random selection of 55 configurations among the low energy ones (we have taken the lowest energy configuration found as the zero of energy). Notice that the initial configuration is not included in the graph as its total energy is well above those values. Six of these configurations are shown in figure 5(b). In the supplementary data (available at stacks.iop.org/Nano/20/264015) we include an animated gif with the ball-and-stick models of the 55 structures. Notice that total energy differences among all of the displayed configurations are lower than 3 eV. Considering that just the atoms in the pyramid and in the first slab layer $(50 + 64 = 114$ atoms, out of the 242 atoms that are allowed to move during the search process) contribute significantly to the energy change, the largest energy difference per atom is smaller than 0.03 eV. Thus, all of the low energy configurations shown in figure 5(a) are accessible, even at room temperature, and can be considered as possible tip structures.
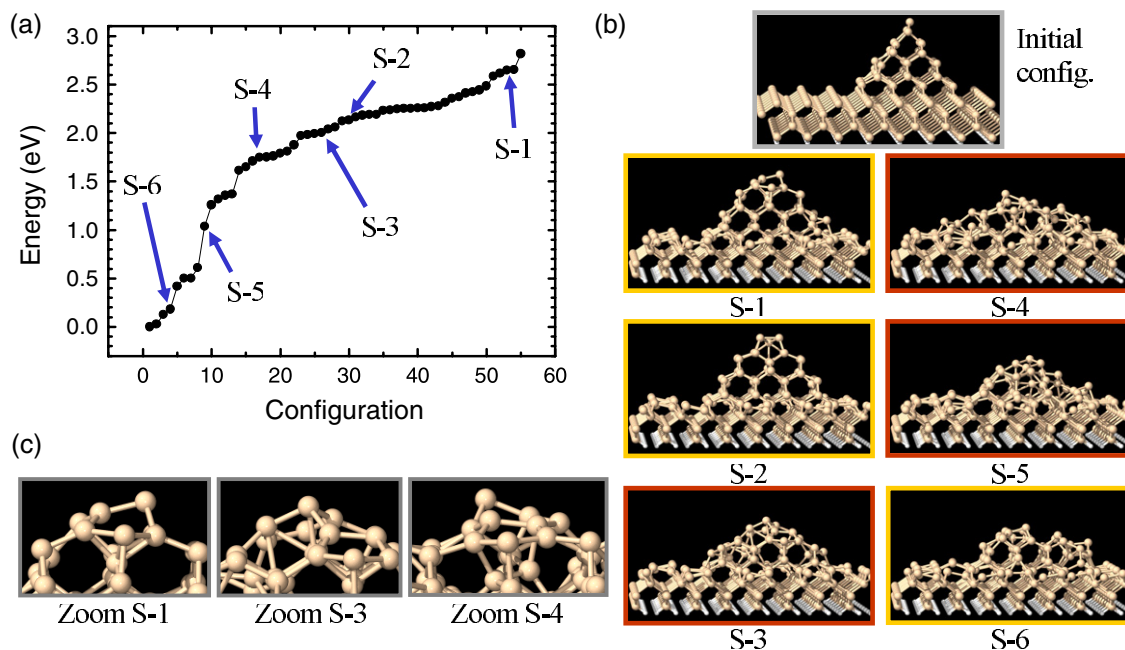
Figure 5. Minima hopping method results. (a) Energy of selected low energy configurations. The selection has been randomly done between the 12000 low energy local minima that the calculation has visited. We have chosen the configuration with the lowest energy as the reference. (b) Ball-and-stick model of the initial configuration (its energy is not shown in (a) because it is too high) and another six configurations. Crystalline structures (S-1, S-2 and S-6) are marked by a yellow border and amorphous tips (S-3, S-4 and S-5) are marked by a red one. A movie with the 55 selected configurations is available in supplementary data (available at stacks.iop.org/Nano/20/264015). (c) Zoom of the terminations of configurations S-1, S-3 and S-4. We can identify the T4 or dimer structures.

To test the apex structures obtained with the minima hopping method, we have calculated the interaction of the selected configurations with the same cluster that simulates a Si surface ad-atom used in the study of the small nanoasperities in section 3.1 (shown in the inset of figure 1(b)). For these calculations, we want to use the first principles DFT method, Fireball [30], in order to provide a fair comparison with the results presented in previous sections. The tip structures found with the minima hopping method are still too large for the DFT method. To reduce the number of atoms, we have kept the tip and the first Si slab layer, cutting out the rest of the system and saturating the dangling bonds of this Si layer with hydrogen atoms (see, for example, the initial structure of figure 7). These atoms are kept fixed during the subsequent DFT calculations. If necessary, we have rotated the tip to produce an atomically sharp apex. Figure 6 shows the force versus distance curves for these configurations. We also include, for comparison, the interaction produced by the T4 and dimer small apexes. All of the tip structures produce forces in the range found for the small nanoasperities and would produce stable imaging (see the discussion in section 3.1). The S2 structure somewhat departs from this behaviour. This structure has been rotated in order to have an apex with the right orientation and exposes a significantly larger surface area than other tips. The discontinuity found in the force curve reflects changes in the structure of these surface areas, induced by the tip–sample interaction, that do not affect the tip apex. These kinds of processes have been proposed as a source of energy dissipation [45, 46].

Once we have confirmed the reliability of the tip configurations found by the minima hopping method, we can
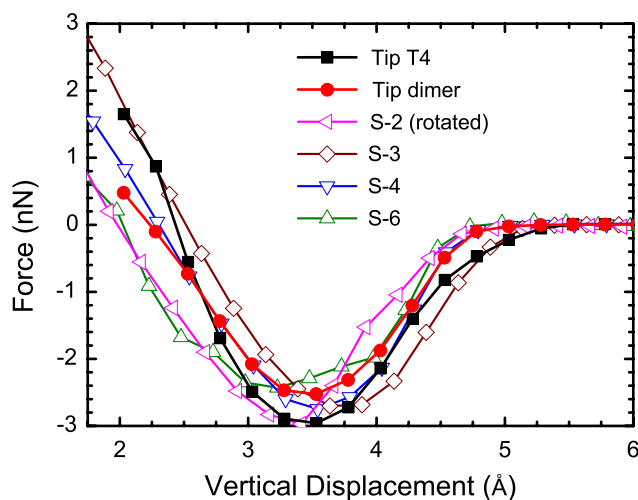
Figure 6. Force as a function of the separation for the interaction between a cluster that simulates a Si ad-atom and the tips obtained from S-2 (open magenta left-triangles), S-3 (open brown diamonds), S-4 (open blue down-triangles) and S-6 (open green up-triangles). We also plot the force for the T4 small tip (solid black squares) and the dimer small tip (solid red circles). As the calculations have been done with DFT, the large structures obtained from the minima hopping calculation have been cut and also, in the S-2 case, rotated.

use them to answer the three specific questions posed in the introduction in order to characterize the real tips used in the experiments. The first question we have to address is the structure of the outermost atoms in the tip apex. Figure 5(c) displays a detailed view of the apex termination for three
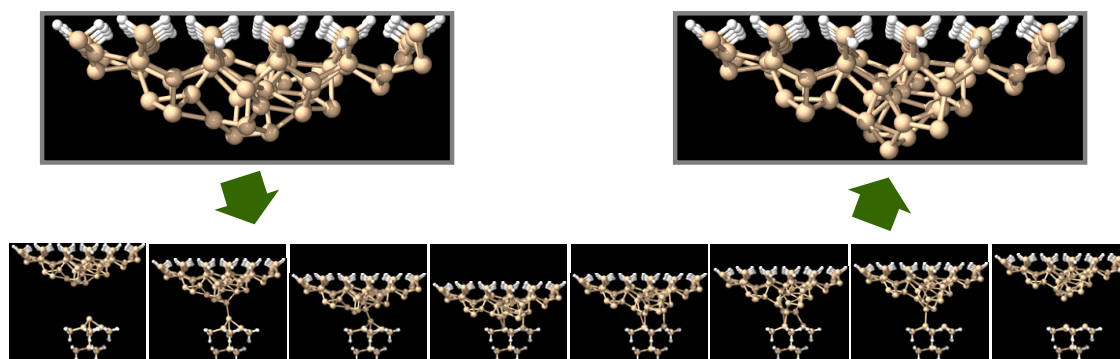
Figure 7. Ball-and-stick models of a possible sharpening process produced by interaction between the tip and the surface. A flat tip becomes atomically sharp after a small indentation over a Si cluster that simulates a surface ad-atom. In this case, the tip has picked up the 'ad-atom' producing the atomic protrusion needed to get atomic resolution. The simulation has been done with Fireball. A movie is available in the supplementary data (available at stacks.iop.org/Nano/20/264015).

different configurations. Again, we find structures that can be identified as T4 or dimer tips. For example, the termination of the S-3 tip is identical to a T4 type structure, while the apexes of the S-1 and S-4 configurations can be clearly labelled as dimer tips. These terminations are also found in many other configurations obtained with the MHM. We have found some configurations terminated by atoms with two dangling bonds (see the initial configuration in figure 5(b)). This particular structure has been proposed to explain the subatomic resolution found in the Si(111)-7 × 7 reconstruction [21]. However, these configurations are systematically higher in energy than other less reactive structures with only one dangling bond (the T4, H3 or dimer terminations). In particular, none of the low energy configurations calculated with the MHM shows the 2-dangling bond termination. Moreover, this termination is unstable under small mechanical deformations or thermal diffusion at RT. We have estimated the energy barrier between the 2-dangling bond structure and the 1-dangling bond structures: our Fireball calculations show that the barrier is lower than 0.2 eV. Therefore, our results indicate that the 2-dangling bond termination is not stable under normal operation conditions. However, the experiments on subatomic resolution [21] were conducted with very small cantilever amplitudes and a very strong applied electrostatic field normal to the surface. These particular conditions might change the relative stability, but this study is out of the scope of this work.

In the next step of our analysis, we focus on the structure of the intermediate layers, those joining the outermost atoms with the rest of the tip. In particular, we want to determine if the structure of these layers is crystalline, as for the bulk continuation we assume in the small nanoasperities, or amorphous, as we have found in Si clusters. The optimal, low energy MHM configurations presented in figure 5 suggest that both structures, crystalline and amorphous, are possible. Just considering the selected tips of figure 5(b), three low energy configurations (S-1, S-2 and S-6) could be considered as crystalline, while the other three (S-3, S-4 and S-5) have, at least, an atom with a coordination number larger than 4 leading to a disordered, amorphous-like apex (very easy to see in the S-5 tip). These results confirm that the order of these intermediate

layers does not have a significant influence on the structures appearing right at the tip apex.

Our last question concerns the sharpening process. In order to get atomic resolution the tip should be atomically sharp. The different steps in the tip preparation process, from the cleaning procedure to intentional contact with the surface to be studied, can play a role. *A priori*, it seems reasonable to assume that energetic and thermodynamic considerations (the effect of the temperature) would favour blunter tips, while the tip–sample interaction would yield sharper apexes. A recent DFT calculation with rather small apexes [40] shows the interest and also the difficulty of the simulation of this process.

A complete characterization of sharpening is beyond the aim of this work. However, our simulations can shed light on the contribution of the different factors. Regarding the energetic considerations, our simulations support that atomically sharp tips are stable under normal conditions (i.e., room temperature). Several configurations of all of the systems we have simulated, from the small nanoasperities to the larger system, show tip terminations with atomic protrusions. Moreover, the energy of these configurations is not significantly different from the one of the blunt tip structures. These results seem to be independent of the boundary conditions or the method of calculation. Thus, we can conclude that purely thermodynamic considerations do not result in a significant bias to either sharp or blunt tip apexes.

We have also simulated, using Fireball and one of the tip structures found in the MHM search, a possible process of tip sharpening. We have softly indented and retracted a blunt tip apex against the small cluster which simulates a Si ad-atom that we have used to characterize the tip–surface interaction. After the indentation, the tip termination is atomically sharp. The process can be seen in figure 7 or in an animated gif included in the supplementary data (available at stacks.iop.org/Nano/20/264015). In this particular case, the sharpening is associated with the tip picking up an atom from the cluster that simulates the surface. We expect this process to scale up with the tip size and the indentation depth. In a more realistic situation, we can envision the significant contamination of the tip with surface material and the formation of a stable apex. This kind of process would explain,

from a more fundamental perspective, our ability to reproduce quantitatively experimental force curves on Ge surfaces with calculations based on Ge nanoasperities [28]. Unfortunately, this simulation is beyond the current capabilities of DFT methods, even the Fireball code, and multiscale or accurate semiclassical methods would be necessary for this task.

4. Conclusions

In summary, we have provided a detailed, atomistic description of the semiconductor tip apexes that can provide atomic resolution in AFM experiments on semiconductor surfaces. We have performed simulations for systems with different sizes and boundary conditions, using different theoretical methodologies in order to characterize the relevant structures for the outermost tip atoms, that control the tip–sample interaction and thus are the ones responsible for imaging and manipulation. Our results confirm that the atomically sharp terminations (e.g. the T4, H3 or dimer structures) introduced in previous works [2–4, 25, 28], are indeed representative of the apex structure we can expect after the tip preparation process. We have also shown that the order (either amorphous or crystalline) of the intermediate layers (those joining the outermost atoms to the rest of the tip) does not have a significant influence on the apex structures. Finally, we have shown that the atomically sharp tips providing the atomic resolution can be expected in real tips and are stable under normal operation conditions. We have also illustrated a possible sharpening process mediated by the tip–surface interaction, which helps to produce an atomic protrusion on an initially blunt tip, but more work is definitely needed in order to characterize this process. Although our simulations have focused on Si tips, given the similarity among different semiconductor materials, we expect these conclusions to be applicable to AFM experiments involving semiconductor surfaces, where the tip is likely contaminated with surface material.

Acknowledgments

References

[1] Morita S, Wiesendanger R and Meyer E 2002 Noncontact atomic force microscopy *NanoScience and Technology* (Berlin: Springer)

[2] García R and Pérez R 2002 Dynamic atomic force microscopy methods *Surf. Sci. Rep.* **47** 197–301

[3] Giessibl F J 2003 Advances in atomic force microscopy *Rev. Mod. Phys.* **75** 949–83

[4] Pérez R, Payne M C, Štich I and Terakura K 1997 Role of covalent tip–surface interactions in noncontact atomic force microscopy *Phys. Rev. Lett.* **78** 678–81

[5] Pérez R, Štich I, Payne M C and Terakura K 1998 Surface–tip interactions in noncontact atomic-force microscopy on reactive surfaces: Si(111) *Phys. Rev.* B **58** 10835–49

[6] Lantz M A, Hug H J, Hoffmann R, van Schendel P J A, Kappenberger P, Martin S, Baratoff A and Güntherodt H-J 2001 Quantitative measurement of short-range chemical bonding forces *Science* **291** 2580–3

[7] Hoffmann R, Kantorovich L N, Baratoff A, Hug H J and Güntherodt H-J 2004 Sublattice identification in scanning force microscopy on alkali halide surfaces *Phys. Rev. Lett.* **92** 146103

[8] Abe M, Sugimoto Y, Custance O and Morita S 2005 Room-temperature reproducible spatial force spectroscopy using atom-tracking technique *Appl. Phys. Lett.* **87** 173503

[9] Hölscher H, Langkat S M, Schwarz A and Wiesendanger R 2002 Measurement of three-dimensional force fields with atomic resolution using dynamic force spectroscopy *Appl. Phys. Lett.* **81** 4428–30

[10] Abe M, Sugimoto Y, Namikawa T, Morita K, Oyabu N and Morita S 2007 Drift-compensated data acquisition performed at room temperature with frequency modulation atomic force microscopy *Appl. Phys. Lett.* **90** 203103

[11] Loppacher C, Bennewitz R, Pfeiffer O, Guggisberg M, Bammerlin M, Schär S, Barwich V, Baratoff A and Meyer E 2000 Experimental aspects of dissipation force microscopy *Phys. Rev.* B **62** 13674–9

[12] Hug H J and Baratoff A 2002 *Noncontact Atomic Force Microscopy* (Berlin: Springer) chapter 20 pp 395–432

[13] Oyabu N, Custance O, Yi I, Sugawara Y and Morita S 2003 Mechanical vertical manipulation of selected single atoms by soft nanoindentation using near contact atomic force microscopy *Phys. Rev. Lett.* **90** 176102

[14] Sugimoto Y, Abe M, Hirayama S, Oyabu N, Custance O and Morita S 2005 Atom inlays performed at room temperature using atomic force microscopy *Nat. Mater.* **4** 156–9

[15] Sugimoto Y, Jelinek P, Pou P, Abe M, Morita S, Perez R and Custance O 2007 Mechanism for room-temperature single atom lateral manipulation on semiconductors using dynamic force microscopy *Phys. Rev. Lett.* **98** 106104

[16] Sugimoto Y, Pou P, Custance O, Jelinek P, Abe M, Perez R and Morita S 2008 Complex patterning by vertical interchange atom manipulation using atomic force microscopy *Science* **322** 413–7

[17] Hirth S, Ostendorf F and Reichling M 2006 Lateral manipulation of atomic size defects on the CaF$_2$(111) surface *Nanotechnology* **17** S148–54

[18] Nishi R, Miyagawa D, Seino Y, Yi I and Morita S 2006 Non-contact atomic force microscopy study of atomic manipulation on an insulator surface by nanoindentation *Nanotechnology* **17** S142–7

[19] Sugimoto Y, Pou P, Abe M, Jelinek P, Perez R, Morita S and Custance O 2007 Chemical identification of individual surface atoms by atomic force microscopy *Nature* **446** 64–7

[20] Ke S H, Uda T, Štich I and Terakura K 2001 First-principles simulation of atomic force microscopy image formation on a GaAs(110) surface: effect of tip morphology *Phys. Rev.* B **63** 245323

[21] Giessibl F J, Hembacher S, Bielefeldt H and Mannhart J 2000 Subatomic features on the silicon (111)-(7 × 7) surface observed by atomic force microscopy *Science* **289** 422

[22] Hembacher S, Giessibl F J and Mannhart J 2004 Force microscopy with light-atom probes *Science* **305** 380

[23] Livshits A I, Shluger A L, Rohl A L and Foster A S 1999 Model of noncontact scanning force microscopy on ionic surfaces *Phys. Rev. B* **59** 2436–48

[24] Foster A S, Barth C, Shluger A L and Reichling M 2001 Unambiguous interpretation of atomically resolved force microscopy images of an insulator *Phys. Rev. Lett.* **86** 2373–6

[25] Hofer W A, Foster A S and Shluger A L 2003 Theories of scanning probe microscopes at the atomic scale *Rev. Mod. Phys.* **75** 1287–331

[26] Foster A S, Gal A Y, Gale J D, Lee Y J, Nieminen R M and Shluger A L 2004 Interaction of silicon dangling bonds with insulating surfaces *Phys. Rev. Lett.* **92** 036101

[27] Abe M, Sugimoto Y, Custance O and Morita S 2005 Atom tracking for reproducible force spectroscopy at room temperature with non-contact atomic force microscopy *Nanotechnology* **16** 3029–34

[28] Oyabu N, Pou P, Sugimoto Y, Jelinek P, Abe M, Morita S, Pérez R and Custance O 2006 Single atomic contact adhesion and dissipation in dynamic force microscopy *Phys. Rev. Lett.* **96** 106101

[29] Sugimoto Y, Pou P, Custance O, Jelinek P, Morita S, Pérez R and Abe M 2006 Real topography, atomic relaxations, and short-range chemical interactions in atomic force microscopy: the case of the α-Xn / Si(111)-($\sqrt{3} \times \sqrt{3}$) $r30°$ surface *Phys. Rev. B* **73** 205329

[30] Jelinek P, Wang H, Lewis J P, Sankey O F and Ortega J 2005 Multicenter approach to the exchange–correlation interactions in *ab initio* tight-binding methods *Phys. Rev. B* **71** 235101

[31] Hohenberg P and Kohn W 1964 Inhomogeneous electron gas *Phys. Rev.* **136** B864–71

[32] Kohn W and Sham L J 1965 Self-consistent equations including exchange and correlation effects *Phys. Rev.* **140** A1133–8

[33] Lewis J P, Glaesemann K R, Voth G A, Fritsch J, Demkov A A, Ortega J and Sankey O F 2001 Further developments in the local-orbital density-functional-theory tight-binding method *Phys. Rev. B* **64** 195103

[34] Sankey O F and Niklewski D J 1989 *Ab initio* multicenter tight-binding model for molecular-dynamics simulations and other applications in covalent systems *Phys. Rev. B* **40** 3979–95

[35] Perdew J P and Zunger A 1981 *Phys. Rev. B* **23** 5048

[36] 1999 *CASTEP 4.2 Academic Version* Licensed under the UKCP-MSI Agreement Payne M C, Teter M P, Allan D C, Arias T A and Joannopoulos J D 1992 *Rev. Mod. Phys.* **64** 1045–97

[37] Goedecker S 2004 Minima hopping: an efficient search method for the global minimum of the potential energy surface of complex molecular systems *J. Chem. Phys.* **120** 9911–7

[38] Lenosky T J, Kress J D, Kwon I, Voter A F, Edwards B, Richards D F, Yang S and Adams J B 1997 Highly optimized tight-binding model of silicon *Phys. Rev. B* **55** 1528–44

[39] Perdew J P, Burke K and Ernzerhof M 1996 Generalized gradient approximation made simple *Phys. Rev. Lett.* **77** 3865–8

[40] Caciuc V, Hölscher H, Blügel S and Fuchs H 2006 Atomic-scale sharpening of silicon tips in noncontact atomic force microscopy *Phys. Rev. Lett.* **96** 016101

[41] Baletto F and Ferrando R 2005 Structural properties of nanoclusters: energetic, thermodynamic, and kinetic effects *Rev. Mod. Phys.* **77** 371

[42] Ho K-M, Shvartsburg A A, Pan B, Lu Z-Y, Wang C-Z, Wacker J G, Fye J L and Jarrold M F 1998 Structures of medium-sized silicon clusters *Nature* **392** 582

[43] Röthlisberger U, Andreoni W and Parrinello M 1994 Structure of nanoscale silicon clusters *Phys. Rev. Lett.* **72** 665–8

[44] Kaxiras E and Jackson K 1993 Shape of small silicon clusters *Phys. Rev. Lett.* **71** 727–30

[45] Hoffmann R, Baratoff A, Hug H J, Hidber H R, Löhneysen H v and Güntherodt H-J 2007 Mechanical manifestations of rare atomic jumps in dynamic force microscopy *Nanotechnology* **18** 395503

[46] Alireza Ghasemi S, Goedecker S, Baratoff A, Lenosky T, Meyer E and Hug H J 2008 Ubiquitous mechanisms of energy dissipation in noncontact atomic force microscopy *Phys. Rev. Lett.* **100** 236106